

Real-Time Internet Distribution of Satellite Products for Tropical Cyclone Reconnaissance



Jeffrey D. Hawkins,* Thomas F. Lee,* Joseph Turk,*
Charles Sampson,* John Kent,+ and Kim Richardson*

ABSTRACT

Tropical cyclone (TC) monitoring requires the use of multiple satellites and sensors to accurately assess TC location and intensity. Visible and infrared (vis/IR) data provide the bulk of TC information, but upper-level cloud obscurations inherently limit this important dataset during a storm's life cycle. Passive microwave digital data and imagery can provide key storm structural details and offset many of the vis/IR spectral problems. The ability to view storm rainbands, eyewalls, impacts of shear, and exposed low-level circulations, whether it is day or night, makes passive microwave data a significant tool for the satellite analyst. Passive microwave capabilities for TC reconnaissance are demonstrated via a near-real-time Web page created by the Naval Research Laboratory in Monterey, California. Examples are used to illustrate tropical cyclone monitoring. Collocated datasets are incorporated to enable the user to see many aspects of a storm's organization and development by quickly accessing one location.

1. Introduction

Passive microwave digital imagery has been proven to significantly aid the global tropical cyclone reconnaissance effort as demonstrated by products developed by the Naval Research Laboratory's (NRL) Marine Meteorology Division. Near-real-time passive microwave (PMW) imagery from both the Special Sensor Microwave/Imager (SSM/I) and the Tropical Rainfall Measuring Mission (TRMM) Microwave Imager (TMI) can be made available within 1–3 h for tropical cyclones worldwide. These storm-centered, high-resolution images readily display evolving storm organization and structure that are not always evident in coincident visible and infrared (vis/IR) imagery.

High cloud decks often obscure vital mid- and low-level cloud signatures within vis/IR images. This obscuration is a serious drawback because vis/IR imagery provides the bulk of the global tropical cyclone (TC) position and intensity information available to forecasters.

The 85-GHz channels on both the SSM/I and TMI sensors are particularly revealing of TC rainband and eyewall mapping. Intense convection within these images is marked by dramatically lowered equivalent blackbody brightness temperatures (T_B) caused by scattering from precipitation-size ice hydrometeors. Fortunately, cirrus canopies, which may cover very large nonraining areas, contain small ice crystals and do not produce signatures on PMW imagery. Thus, the satellite analyst can observe the convective rainbands of each TC to more precisely locate the storm and infer important intensity information (Hawkins et al. 1998a; Velden et al. 1989).

The use and ability to interpret PMW imagery by operational personnel has been limited until recently for several reasons: (a) only one to two SSM/I instruments have been in orbit, limiting spatial/temporal coverage; (b) processing capabilities have been inadequate; (c) bandwidth for distributing data to operational users has been insufficient; and (d) suitable

*Marine Meteorology Division, Naval Research Laboratory, Monterey, California.

+Science Applications International Corporation, Monterey, California.

Corresponding author address: Mr. Jeffrey D. Hawkins, Marine Meteorology Division, Naval Research Laboratory, 7 Grace Hopner Ave., Monterey, CA 93943.

E-mail: hawkins@nrlmry.navy.mil

In final form 28 November 2000.

©2001 American Meteorological Society

hardware/software display capabilities have not always been available. The drawbacks noted above have been mitigated by several developments. Three SSM/I instruments and one TMI sensor are now operational. Adequate processing power has arrived as CPU speeds increase at no additional cost and bandwidth has increased between processing centers and operational users. Finally, the research community has developed integrated hardware/software solutions.

NRL has demonstrated the use of Web technology to remove one of the main obstacles in using PMW for tropical cyclone reconnaissance by providing efficient, broad distribution of near-real-time, storm-centered PMW imagery products (Lee et al. 1999). The Web page uses storm locations from tropical cyclone warning centers via the Automated Tropical Cyclone Forecast System (ATCF) (Sampson and Schrader 2000) to position all satellite products. The Web page, http://kauai.nrlmry.navy.mil/sat-bin/tc_home, can be accessed from any computer with Internet access and a frames-capable browser. Users are presented with a graphical user interface (GUI) that readily permits them to select the storm of interest and view a suite of passive microwave and vis/IR products that are all collocated for each PMW satellite overpass that covers a storm or system (referred to as a "hit"). Background processing algorithms automatically update the Web page with new products as they come online. The Web page also includes the latest TC warning messages and official track forecasts that enable the user to visually see the most recent storm motion, size, and short-term forecasts.

The TC Web page provides an easy to use methodology to distribute important high-resolution PMW imagery that can be used by researchers, students, and operational warning centers. The input satellite datasets will be described in section 2. The data processing and interaction with the ATCF system will be described in section 3. Examples of the Web page layout and usage are depicted in section 4. Data interpretation of the multisensor satellite data products in the TC environment is discussed in section 5. Results and conclusions obtained through operational user feedback are presented in section 6 along with transition plans and future enhancements and capabilities.

2. Satellite datasets

Mounted aboard the polar-orbiting Defense Meteorological Satellite Program (DMSP) spacecraft, the

SSM/I is a passive microwave radiometer, which orbits with a period of 102 min over a swath width of nearly 1400 km. It collects radiation naturally emitted by the surface of the earth and the intervening atmosphere at 19.35, 22.235, 37.0, and 85 GHz. With the exception of 22.235 GHz, all of the channels have vertical (V) and horizontal (H) polarizations (Hollinger 1989). DMSP satellites are sun synchronous, meaning that they image a given earth location at the same local time of day. There are significant gaps between successive passes, especially in the Tropics, limiting storm detection to, at most, twice during a 24-h period by a given satellite. Sometimes only a portion of a storm will be covered. At other times, a storm is in the "blind," meaning that it is not detected by the SSM/I on a particular satellite for a sequence of orbits. Since the DMSP satellites were purposely launched into morning-evening orbits, there is never any coverage during the middle of the day and middle of the night.

Figure 1 depicts the broad coverage of SSM/I 85-GHz data available over a typical 24-h period globally. SSM/I sensors from satellites *F-11*, *F-13*, and *F-14* leave a few elongated coverage gaps shown by the gray patches. The location of these gaps changes daily. Note the high moisture in the Tropics as evidenced by the warm T_b . Frontal bands can be seen in the middle North and South Atlantic basins and dry regions are evident off the northwestern U.S. coast, the Mediterranean Sea, and the Sea of Japan (blue colors).

Figure 2 illustrates the typical number of overpasses at any given location globally for a 24-h period by combining the swaths from these three SSM/I sensors. The color table on the right indicates the deep Tropics often experience one to three passes per day. The frequency of overpasses varies more at 20°N/S, ranging from zero to six per day. Finally, the swath coverage decreases the occurrence of zero or missing data near 40°N/S, but also results in fewer areas near six passes per day. The specific data areas for a given day will change, but the general pattern of coverage persists day to day.

The TRMM satellite, launched in late 1998, is in a much more favorable orbit for tropical cyclone observation than the DMSP constellation of satellites. The TRMM orbit has an inclination of 35°, versus the typical 98° for the National Oceanic and Atmospheric Administration and DMSP polar orbiters. The tropical inclination angle and non-sun-synchronous orbit enables the TRMM satellite to provide excellent temporal sampling for tropical rain, its primary mission. The orbital characteristics permit TRMM to fill in some

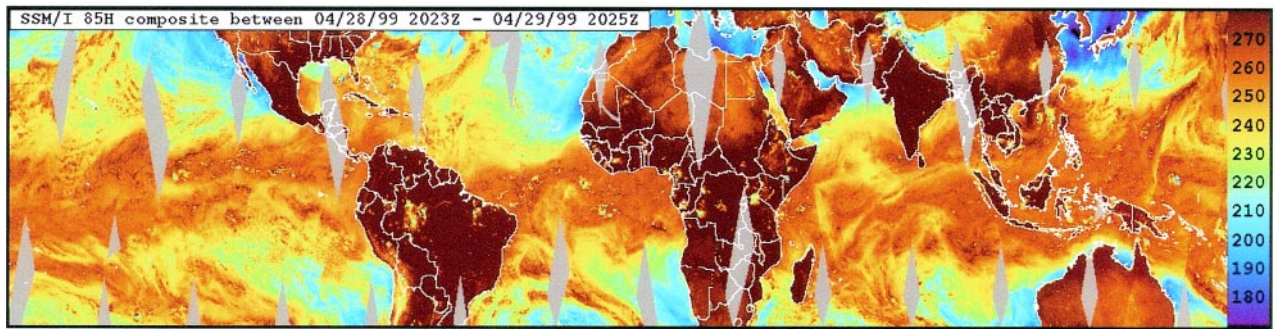


FIG. 1. A 24-h global composite of 85-GHz H-pol brightness temperatures using data from *F-11*, *F-13*, and *F-14* SSM/I sensors during 28–29 Apr 1999. Color temperature scale shows colder values in blue and warmer temperatures in yellow, orange, and brown. Note that only a few gaps remain by combining multiple sensors.

of the temporal gaps left by the SSM/I sensors. One TMI can provide one to two overpasses per storm each day. At the present there is only one TRMM satellite; however, in the future, a cluster of eight satellites could reliably provide storm images every 3 h (Simpson et al. 1998).

The TMI sensor uses nearly identical frequencies as the SSM/I with the major addition of a dual-polarized 10.7-GHz channel. Flying low, at about one-half the altitude of DMSP, the TRMM TMI has an effective field of view of $7 \text{ km} \times 5 \text{ km}$ at 85 GHz (Kummerow et al. 1998), compared to $16 \text{ km} \times 14 \text{ km}$ for SSM/I. The swath width for the TMI is 760 km (Simpson et al. 1996). The TMI's higher spatial resolution is especially helpful in derived products such as rain rate and wind speed (Hawkins et al. 1999).

Figure 3 shows the increased availability of passive microwave data from 40°N to 40°S when TMI data are added to the SSM/I data presented in Fig. 2. TMI data provide enhanced coverage not only in the deep Tropics but also between 30° and 38°N as the number of combined overpasses reaches 9 to 10 per

day. Thus, even with the relatively small TMI swath (780 km), the coverage is enhanced. This result is significant in terms of reducing the time gaps that previously existed with SSM/I-only datasets.

There are important interchannel variations in the degree to which clouds and precipitation scatter, absorb, and emit passive microwave energy at TMI and SSM/I frequencies. At the higher frequencies, scattering by precipitation-sized ice particles can depress T_B significantly, particularly at 85 GHz. Scattering from raindrops can also depress 85-GHz T_B to a smaller degree, especially over deep, moist cloud systems. The scattering property of hydrometers makes 85 GHz particularly useful to observe the convective structure of tropical cyclones (Spencer et al. 1989). Away from deep convection, emission from shallow clouds, warm rain (no ice processes), and significant low-level water vapor will cause 85-GHz T_B to increase against a radiometrically cold ocean background. Passive microwave signatures at 85 GHz often represent a combination of emission and scattering effects. However, on 85-GHz images, it is usually possible to distinguish

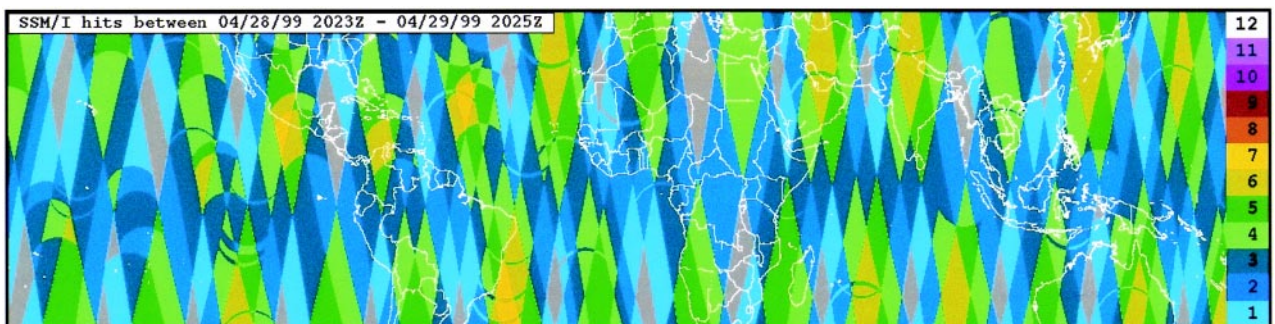


FIG. 2. Number of SSM/I swaths for 24-h period during 28–29 Apr 1999. The color bar on the right maps the number of swaths that cover a given geographic area around the globe. The display represents the domain from 40°N to 40°S . The plot reveals few hits near the equator by any of the three SSM/I sensors, while coverage increases by a factor of 3–4 toward the midlatitudes. Note the inclination of SSM/I swaths.

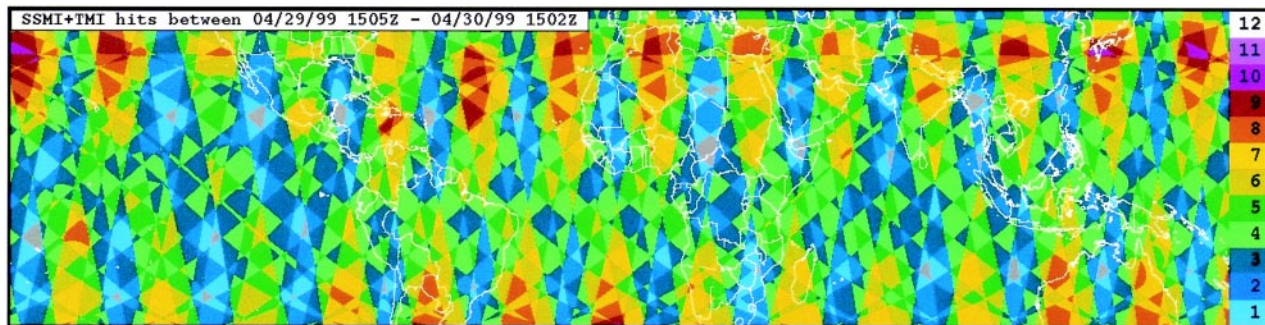


FIG. 3. Combined number of SSM/I and TMI swaths during a 24-h period. The plot shows both ascending and descending orbits and clearly illustrates the 35° inclination of the TRMM satellite, with coverage extending to 38°N and S (note demarcation line).

deep convection (depressed T_b) from the combined effects of water clouds, water vapor, and warm rain (all elevated T_b). Precipitation-sized particles induce scattering to a lesser degree at the other SSM/I and TMI frequencies, but these signatures are more difficult to detect in images. At the lower frequencies the emission signatures dominate over the scattering signatures such that all precipitation generally appears as “warm” against a “cold” ocean background.

Interpretation of 85-GHz images (either polarization) suffers from one major ambiguity. In regions just beyond the influence of tropical cyclones, water vapor, cloud water, and convection are diminished. The low-emissivity sea surface, seen through these relatively transparent atmospheres, is associated with relatively low T_b . Thus, when viewing images, this sea surface can be mistaken as cold convection and vice versa. To correct for possible misinterpretations, we compute a polarization-corrected temperature (PCT) based on the horizontal and vertical polarization of (Spencer et al. 1989).

The PCT is an excellent indicator of convective precipitation and correlates well with lightning flashes over land (Mohr et al. 1996). In PCT images, T_b lower than about 255 K indicate precipitation. The PCT corrects T_b over problematic regions of low moisture to represent the relatively high temperatures of the near-surface atmosphere. Thus, the PCT allows a way to distinguish between deep convection and adjacent convection-free regions. Since the 85-GHz frequencies are identical on the TMI and SSM/I sensors, as are the view angles, interpretation of the 85-GHz PCT product is the same for both.

Unfortunately, compared to raw 85-GHz images (V and H), the PCT image has its own limitation: it nearly eliminates the contrast between low-level vapor, clouds, rain, and/or the adjacent cloud-free ocean. To combine the best aspects of the PCT and uncor-

rected 85-GHz images, we derive a color-blended image (Table 1). The effect of the PCT is to make convective precipitation appear red in this image. The two uncorrected 85-GHz channels combine to make low-level cloud water appear as blue-green. Cloud-free regions become gray or black over the ocean. These images show precipitation above the freezing level as red, and low-level phenomena (water clouds, water vapor, and light rain) as blue-green. Precipitating convection (red) and the sea surfaces (black or gray) can now be distinguished from one another (example shown later in Fig. 7). This technique is similar to the “false color” images of tropical convection produced by Negri et al. (1989), who included 85-GHz (V and H) and 37-GHz (V) data in a three-color combination.

By combining the various channels of the SSM/I or TMI, we can produce and display a variety of geophysical products that are useful for TC analysis and prediction. Rain rate (Ferraro 1997), integrated precipitable water (Alishouse et al. 1990), and ocean surface wind speed (Goodberlet et al. 1990) are created for each TC overpass at nominal 25-km resolution. Images at higher spatial resolution are produced via remapping, with some limitations as noted in section 3. Channel combinations are applied to TMI data to produce a similar set of geophysical products as for the SSM/I. At this time we display rain rate and cloud liquid water products resident in the data stream we receive from the National Aeronautics and Space Administration Goddard Space Flight Center (NASA GSFC) TRMM Science Data Information System (TSDIS) as well as a wind speed calculated using the algorithm of Connor and Chang (2000).

However, for observation of tropical cyclone structure, images of the higher-frequency T_b are typically more useful than the derived geophysical parameters. In particular, images of the 85-GHz channels (12.5-km resolution) resolve detail not seen by other SSM/I

channels or channel combinations. Like SSM/I, the TMI 85-GHz channels yield particularly valuable images over tropical cyclones. Thus, as will be illustrated in section 4, the lower-frequency images on the TRMM are also potentially valuable, since they possess sufficient horizontal resolution to show important detail of storm eyes and rainband features.

3. Data processing

SSM/I data arrive at NRL from the Fleet Numerical Meteorology and Oceanography Center (FNMOC) in Monterey, California. TMI data arrive from the TSDIS team. Processing is initiated by looping through a “sector file” of storm centerpoints (Fig. 4). The sector file is updated by routine warning messages and whenever each center determines conditions warrant. Warning messages for the north Indian, western North Pacific, and Southern Hemisphere basins originate from the Joint Typhoon Warning Center (JTWC) located in Hawaii. The central pacific warnings are prepared at the Central Pacific Hurricane Center and reformatted by the Naval Pacific Meteorology and Oceanography Center also in Hawaii. For the eastern North Pacific east of 140°W and the North Atlantic, the messages come from the National Hurricane Center (NHC) in Miami, Florida, via the Naval Atlantic Meteorology and Oceanography Center in Norfolk, Virginia.

NRL has been demonstrating a capability for the operational customer to activate additional product displays over “invest” areas. Invest areas are regions where satellite and/or other observations indicate the potential for TC development or genesis in the near future. These regions contain weak disturbances for

TABLE 1. Scaling for 85-GHz color combination product.

Channel	85-GHz (V) blue	85-GHz (H) green	85-GHz PCT
Range (T_B K)	270–290	240–300	220–310
Tonality	Positive	Positive	Inverse

which official storm numbers or names have not been issued. Both the SSM/I and TMI passive microwave images are highly desirable in these regions to assist in understanding the meteorological environment. These invest areas can be automatically activated by both JTWC and NHC 24 h day⁻¹, a capability that has proven quite beneficial based on comments from the warning centers. Transition of this functionality to FNMOC is under way.

If an arriving microwave pass covers a particular storm, storm-centered passive microwave images are remapped into a Mercator image projection (1600 km on a side). For storms or invest regions that appear in the sector file for the first time, the system reprocesses

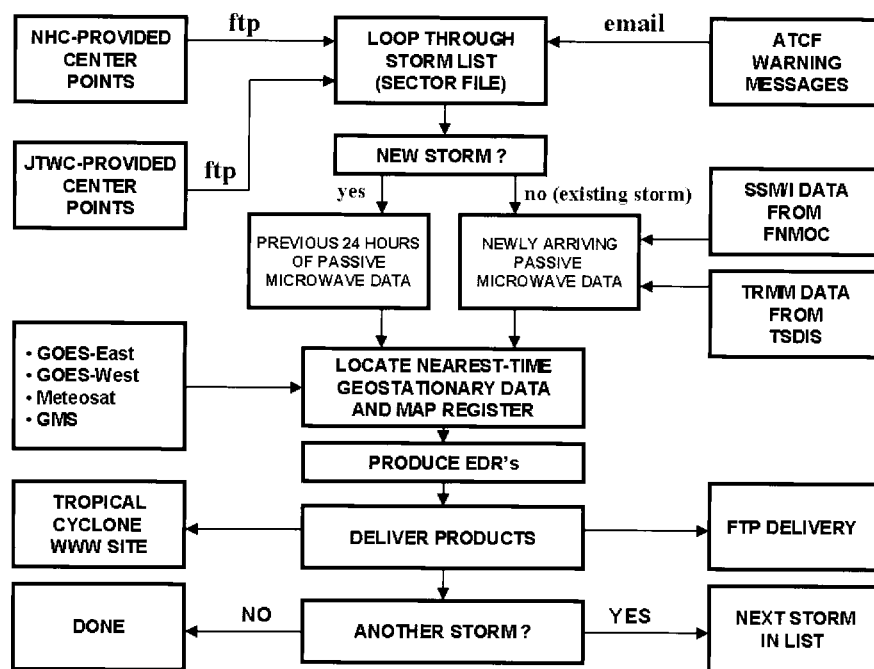


FIG. 4. Flow chart showing the inputs and processing incorporated by the NRL-MRY tropical cyclone Web page. Worldwide TC locations are provided via inputs from NHC and JTWC via warning summaries and other specific requests. Processing programs use each storm's latitude–longitude to process coincident PMW data. Once a hit occurs and time/coverage criteria are satisfied, geostationary vis/IR imagery are created and posted to the Web. Geostationary data from *GOES-8/10*, *GMS-5*, and *Meteosat-5* are added to global SSM/I and TMI data (via FNMOC and NASA GSFC, respectively) to permit multisensor data fusion.

all SSM/I and TMI datasets available within the past 24 h. All PMW products are remapped to 2-km resolution since comparisons with vis/IR data show excellent agreement (Hawkins et al. 1998b). In this way, useful sets of recent images are generated to observe storm genesis. To supplement the passive microwave images, corresponding geostationary images are produced. The geostationary data and passive microwave datasets are both stored in Terascan Data Format, which facilitates subsequent collocation of images. The geostationary data that are nearest in time and place to the microwave storm coverage are mapped into the identical Mercator projection. The PMW products appear approximately 1–3 h after the spacecraft images are acquired. The visible images have spatial resolutions of 1–2 km and the IR images are typically near 4 km. The availability of vis/IR images permits comparisons with PMW images and enhances information extraction from both datasets.

To support this task, NRL Monterey (NRL-MRY) maintains current databases of *Geostationary Operational Environmental Satellite-8 (GOES-8)* over the western Atlantic Ocean, *GOES-10* over eastern/central Pacific Ocean, *Geostationary Meteorological Satellite-5 (GMS-5)* over the western Pacific Ocean and eastern Indian Ocean, *Meteosat-5* over the Indian Ocean, and *Meteosat-7* over Africa and the eastern Atlantic. Our matching of the place/time of a passive microwave pass with corresponding geostationary scenes produces time discrepancies of around 30 min or less. During the daytime, the system outputs high-resolution visible (~1 km sensor resolution) images. At night, when no visible data are available, the system substitutes a bispectral “low cloud” GOES product for storms viewed by either GOES satellite. The product is based on the difference between the long-wave and shortwave infrared channels and shows boundary layer cloud systems, which are often difficult to detect in stand-alone infrared images (Lee et al. 1997). At all times of day or night, two different infrared enhancements are created (~4–5 km sensor resolution). The first is a linear enhancement, while the second employs the infrared BD enhancement curve used routinely by TC satellite analysts (Dvorak 1984).

4. Web page navigation

The NRL-MRY tropical cyclone Web page enables the user to efficiently view a wealth of satellite-derived products for any storm system. The Web page has a

GUI to view passive microwave and vis/IR images as well as warning information for storms worldwide. If only one storm is active, the page defaults to a GUI that displays a selection of products for that storm. If multiple storms are active, the user chooses the storm of interest after the Web page defaults to the lowest numbered storm/system using a preset basin priority. All products are initially shown in a small thumbnail or browse format to minimize bandwidth needed to decide if the full-size product should be called up for analysis.

Figure 5 shows an example of the tropical cyclone Web page during Tropical Storm Rosa’s journey in the eastern North Pacific. The page is divided into the following areas: 1) left frame, 2) top of main frame, 3) row of SSM/I and TMI products, and 4) main display area. The left frame lists all the active tropical systems sorted by basin. A user clicks on a storm name in the left frame and all subsequent product selections are for that storm. At the top of the left frame are buttons allowing the user to see the current storms “active” or all storms for the selected year in all the basins by selecting “all.” By selecting the “year” button, the user can access storms that occurred during 2000, 1999, 1998, and 1997. All images are online and accessible immediately.

Once a “tropical system” is chosen, the user is presented with a series of selection buttons and a default display that shows a warning graphic (if available) and the latest 1-km vis/IR image. The warning graphic originates at the Department of Defense forecast centers where it is created after viewing and discussing all available forecaster information. Figure 6 shows the warning graphic for Hurricane Georges on 29 September 1999 at 1200 UTC. Included in the warning graphic are the historical 6-hourly track positions, the forecast track for 72 h, gale and hurricane wind radii (if present), and a textual warning label. The textual warning label lists current and forecasted positions and intensities (maximum sustained 1-min average wind speeds) along with forecast dates and times. The warning graphic provides users with a quick overview of the tropical cyclone’s history, current and projected intensity, and a geographical frame of reference. A “legend” for the warning graphic is included in the Web page.

The second row of buttons permits the user to select the desired SSM/I and TMI products for the storm highlighted in the left frame. All PMW products across a given row are collocated and are derived from the same SSM/I or TMI pass. Depending on the geostationary satellite, all collocated vis/IR images are within 30 min of the PMW products. The collocation of

2000 Storms
[All](#) [Active](#) [Year](#)

Atlantic

East Pacific
 • 19E.ROSA

Central Pacific

West Pacific
 • 90W.INVEST
 • 31W.BEBINCA

Indian Ocean

Southern Hemisphere

Disclaimer NRL Monterey Marine Meteorology Division (Code 7500) Tropical Cyclone Page Development Team

Display: [Latest](#) Warn: [Text](#) [Track](#) [ATCF](#) 1 km: [Track & Image](#) [VIS](#) [IR](#) Info: [General](#)

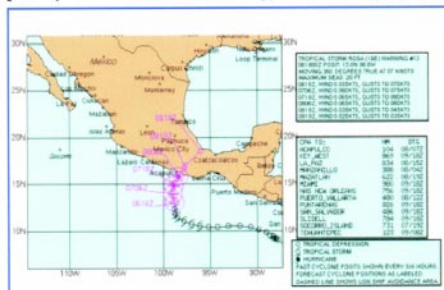
SSM/I Sectors:	VIS	IR	IR-BD	Multi-Sensor	85GHz-H	85GHz-H weak	PCT	Color	Rain	Wind	SSM/I Vapor			
TMI Sectors:	VIS	IR	IR-BD	Multi-Sensor	85GHz-H	85GHz-V	PCT	Color 85	Rain	Wind	Color 37	37GHz-V	37GHz-H	Liquid Water

Latest	Upcoming Passes <small>(more)</small>	Current Time
SSM/I: 11/06 1636Z	/11/07 00:56 F-13 658.4	23:05:41 GMT
TRMM: 11/06 1102Z	/11/07 01:45 trmm 573.0	

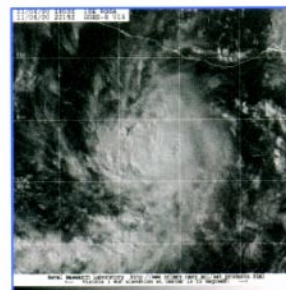
19E.ROSA

Forecast by National Hurricane Center

Graphic by Naval Pacific Meteorology and Oceanography Center



1KM



(Click product for full sized image 21112 Bytes and 197383 Bytes.)

NRL Projects	Home	East Pacific & West Coast	Full-Disk	CONUS	Model Over	Rainrate	Low Cloud	Cloud Tops
	Trop Cyclones	Color Composite	SSM/I-Comp2	Tropics	Cloud Winds	Scatt Winds	Long Movies	Cloud Classification

[Questions or Comments?](#) [Acknowledgements](#)

FIG. 5. Tropical cyclone Web page display of Tropical Storm Rosa in the eastern Pacific on 6 Nov 2000. The graphic on the left shows the previous, current, and forecast track position map provided from ATCF and on the right side is the latest 1-km visible image. The buttons above these two graphics permit the user to view both SSM/I (top row) and TMI (bottom row) images for the selected storm. All products are collocated, including the coincident visible and IR imagery, enabling ready comparison. The leftmost frame indicates there are three active “systems,” two tropical storms and one invest area.

storm-centered products is a unique feature of the NRL-MRY Web page and assists the user in assimilating and interpreting the datasets. The storm-centered products from left to right are (a) visible geostationary images, (b) IR images with normal enhancement, (c) IR images with Dvorak BD enhancement curve, (d) multisensor image that combines geostationary vis/IR and PMW images, (e) 85-GHz H-polarization images with two false color options, (f) PCT (Spencer et al. 1989) image, (g) color composite using PCT and 85-GHz H- and V-polarization images, (h) wind speed, (i) rain rate, (j) total precipitable water in the atmospheric column, and (k) cloud liquid water. Additional 37-GHz products are included for the TMI sensor due to its superior spatial resolution.

The TC Web page allows the user to display the “latest” image or product available. The user can view any earlier product by clicking on the “previous” but-

ton and selecting the desired date/time image. The “mosaic” display mode brings up a gallery of the most recent 16 images or permits the user to select the particular period of date/times desired. This feature makes it easy for researchers to identify good hits and quickly focus on passes that have excellent storm coverage. Several “animation” capabilities enable the user to loop a prescribed sequence of products. Further page details are in the “general” information section in the upper-right-hand corner. Links to numerous other related near-real-time TC-related Web pages can be found on the NHC Web site (<http://www.nhc.noaa.gov/>).

5. Data interpretation

The ability of passive microwave data to significantly enhance an analyst’s view of storm organization

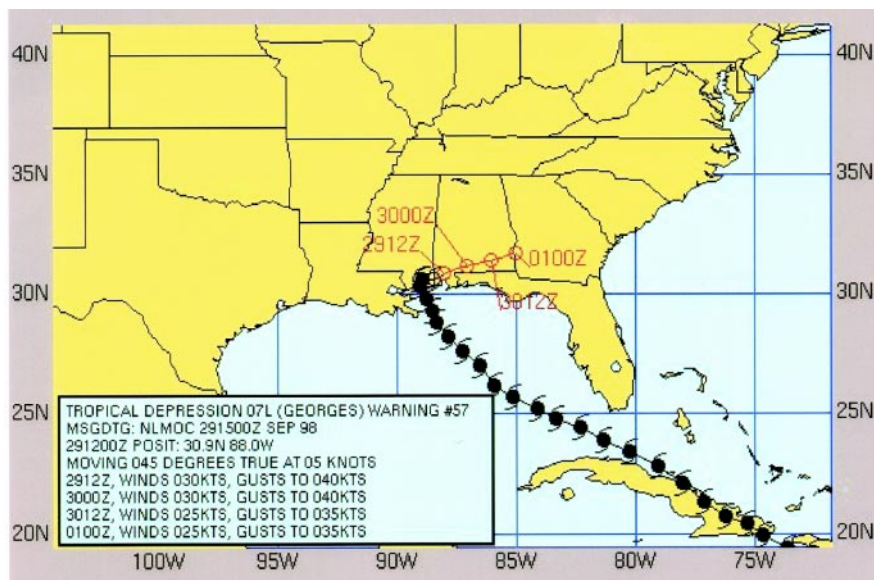


FIG. 6. Warning graphic for Hurricane Georges displaying the preliminary best track in black (filled circles representing hurricane intensity) and the forecast track in red. This graphic always centers a storm's current position and includes the 72-h forecast track. Information on storm intensity forecast is included in lower-left-hand box, indicating the maximum sustained winds/gusts valid during the forecast period.

and structure is illustrated in Fig. 7. This four-panel image of Hurricane Mitch displays a false color enhanced IR image in the upper-left-hand corner. The user can then readily detect the coldest cloud tops, which are typically aligned with the most vigorous convection, though cirrus cloud shields associated with little convection below can confuse interpretation. Figure 7 reveals Mitch does not yet have an eye evident in the IR image, but is becoming better organized and possibly is near the critical stage of hurricane threshold.

The upper-right-hand panel is an enhanced IR image that uses the BD curve lookup table commonly used to determine TC intensity. The BD curve product highlights very cold cloud tops and is used to enable analysts to extract storm intensity using the Dvorak method (Dvorak 1984). The subjective Dvorak technique takes into account the organization of cold (convective) cloud bands, the amount of wrapping around a centroid, their temperature, and evolution of this pattern with time. Tropical cyclone BD curve images can quickly provide a trained analyst with an intensity estimate. Note that no eye is discernable in the IR false colored or BD curve images.

The bottom two panels of Fig. 7 show the ability of the PMW products to reveal a storm eye/center even when this feature is obscured on the IR images (a key

functionality of the NRL-MRY Web page). The lower-left panel is a PCT image that clearly outlines the main rainbands and the enhanced degree of banding around the storm center. In addition, the formation of an eye or center lacking convection/rain can be seen and used to assist in locating the storm center. It is the authors' experience that an eye-like feature will form first in the PMW imagery and then in the vis/IR (Barrett 1999). The early recognition of eye formation afforded by the PMW images is a critical piece of information. Forecasters can use this fact to potentially upgrade tropical cyclone warnings to hurricane/typhoon status many hours earlier than possible if only vis/IR images were available. PMW eye formations need to be correlated

with aircraft data to create the direct link with storm intensities and this effort is currently ongoing.

The 85-GHz PCT has been combined with 85-GHz (V- and H-pol) digital data in the bottom-right-hand panel of Fig. 7. This multichannel product clearly depicts the banding associated with a hurricane as the rainbands are consolidating into two major spiral bands surrounding the rain-free eye. Understanding this rainband structure is a key element in determining whether the system is weakening, remaining steady state, or increasing in intensity. The combination of the IR and SSM/I data in Fig. 7 tells the analyst that the storm is intensifying at this time and an eye may soon appear in IR imagery. In the meantime, the SSM/I data can be used to assist in accurately locating the storm center. This information helps produce more accurate track positions, better initial positions for objective aids, more accurate warning messages, and also helps the definition of TCs in numerical models via vortex bogusing (Goerss and Jeffries 1994).

A time sequence of 85-GHz data can reveal significant TC structural details (Hawkins et al. 1998b; Barrett 1999). The Web page enables this functionality by providing thumbnail versions of up to 16 passive microwave products for any selected storm (provided 16 images exist). Figure 8 demonstrates this

capability for cyclone 02B in the Bay of Bengal. The storm structure continues to improve right up to land-fall and then maintains much of its strength well after landfall. Passive microwave data from the SSM/I and TMI can thus provide crucial details not only while storms are over water but also over land in some

cases. This can be very helpful not only in regions that do not have land-based radars, but also in areas where storm-damaged radars are rendered inoperable.

Passive microwave can be difficult to interpret, especially in the complex tropical cyclone environment. The NRL-MRY Web page includes a “tutorial”

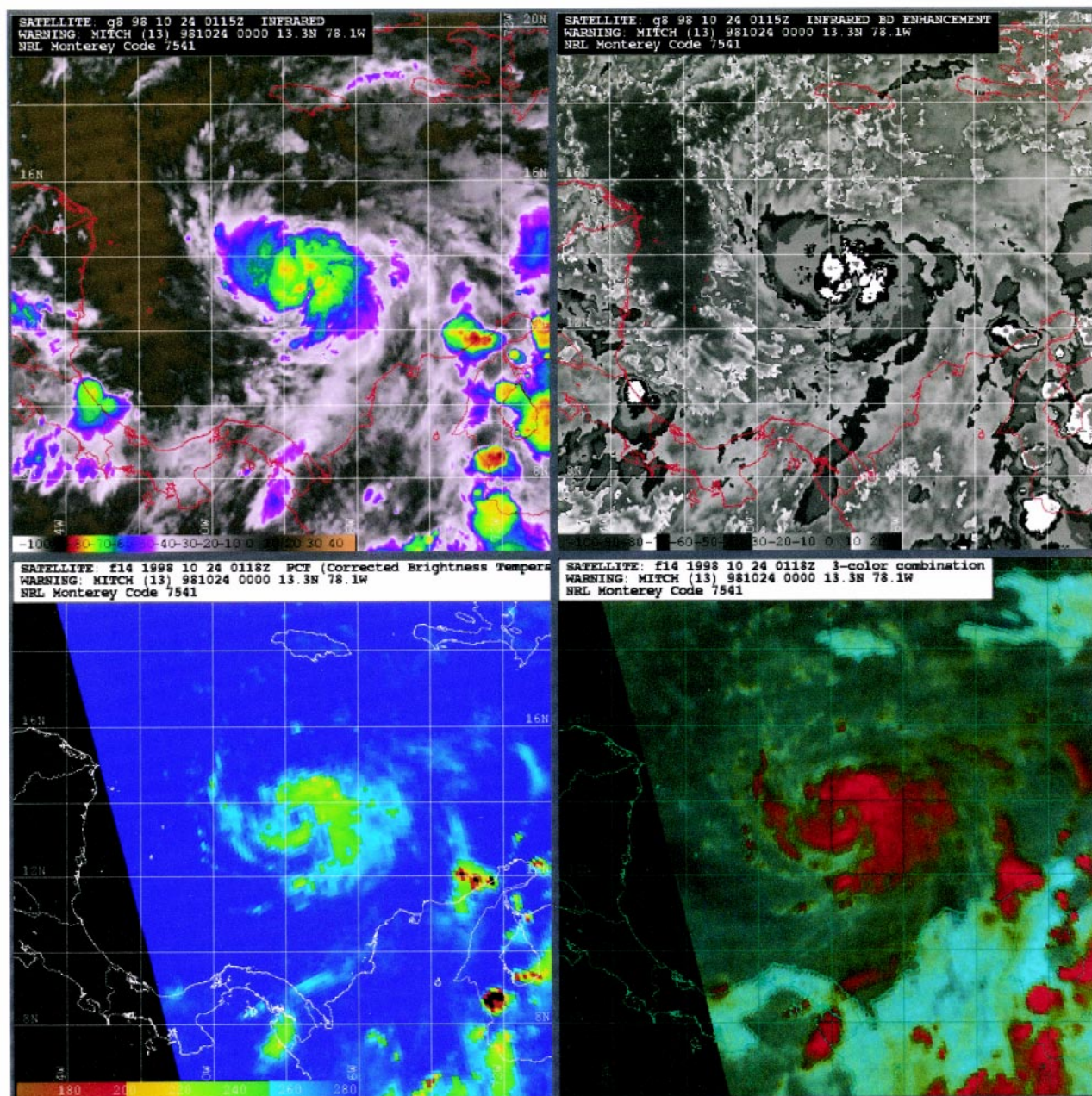


FIG. 7. Multipanel image representing four distinct views of Hurricane Mitch as it gathers strength in the Caribbean Sea at 0118 UTC 24 Oct 1998. Top-left panel is a false color IR image designed to reveal colder (higher) cloud tops according to the color bar in the lower left of that panel's section. Top-right panel is an IR-BD or Dvorak curve enhancement image. Lower-left panel is the PCT image that combines 85-GHz H- and V-pol channels to highlight areas of heavy rain due to scattering/emission. The lower-right panel is a false color composite that uses three inputs: PCT, 85-GHz H-pol, and 85-GHz V-pol. In particular, note the ability of the passive microwave to reveal internal storm structure not evident in the IR imagery, in particular a precipitation-free eye.

section, which appears in the upper-right-hand corner whenever an 85-GHz-based product is displayed. The tutorial includes numerous examples from the Web page and has explanations detailing the features illustrated. The tutorial section has received excellent feedback from training personnel at the warning centers.

All users must recognize that passive microwave limitations exist due to (a) two to eight hits per day does not provide the continuity needed for optimal sampling, (b) near-real-time data is ~1–3 h old since this is stored polar orbiter data (steps are being taken to reduce this by 0.5), and (c) the resolution is not as good as coincident vis/IR data. Many of these factors could be significantly reduced if the Global Precipitation Mission were to reach fruition (Kummerow et al. 2000). Passive microwave datasets are an excellent tool for the TC forecaster/researcher that fills specific needs.

6. Results and conclusions

The NRL-MRY tropical cyclone Web page has enhanced the education and availability of passive microwave imagery/products for TC monitoring around the globe. Passive microwave data are basically a “poor man’s” radar in the sense that one can map the rainbands and TC organization not always seen in visible and IR imagery. Distribution to a large audience of researchers, operational centers, and the general public has increased the awareness of how PMW data can be applied to increase the confidence in TC positioning and intensity estimates. The Internet has enabled NRL to carry out rapid prototyping with a superb feedback mechanism while users make suggestions for improved products and displays.

Operational warning centers such as NHC and JTWC have typically avoided Internet Web sites when obtaining near-real-time data. Original concerns centered on data integrity (accuracy, timeliness, and percent available) as early Web sites suffered from data failures and glitches. However, a host of factors are responsible for making numerous Web sites an automated collection, processing, and distribution center for many data types needed by hurricane forecasters. Reliability has now reached a point where NHC and JTWC routinely use sites such as the one at NRL-MRY in their daily search to assemble key storm characteristics.

The NRL-MRY TC Web page will continue to evolve in several ways. First, the demonstration products will be transitioned to FNMOC for operational implementation. FNMOC will maintain the Web site

24 hours a day and provide enhanced continuity. Second, we will incorporate a new remapping routine for SSM/I data that uses the method described by Poe (1990). Studies at NRL-MRY have indicated improved 85-GHz imagery results for tropical cyclone features when using this interpolation method.

The potential for further enhancements that take advantage of passive microwave data fusion for tropical cyclone monitoring applications is large. A number of new sensors have either been recently launched or will be in place within the next one to three years. The Advanced Microwave Sounding Unit humidity sensor (AMSU-B) is now working on the Earth Observing System (*EOS-AM* or *TERRA* launched in December 1999) and the second in the series is *EOS-PM* or *AQUA* to be launched in mid-2001. AMSU-B (Vangasse et al. 1995) includes a channel at 89.0 GHz with a spatial resolution of 16-km at nadir. Initial images from this sensor have shown promise with regard to mapping TC organization and structure (note that AMSU-B data will complement SSM/I data temporally). In addition, efforts to map the upper-level warm core temperature anomaly using AMSU-A and relate them to storm intensity have made significant progress (Velden and Brueske 1999).

The SSM/I will be followed by the Special Sensor Microwave/Imager Sounder (SSM/IS; Swadley and Chandler 1991) that combines the SSM/I with the T1/T2 temperature and humidity sounders on the DMSP spacecraft. The first SSM/IS launch will be in mid-2001. The collocated imager and sounder channels will make it possible to produce superior geophysical retrievals and more readily permit multichannel PMW TC views, in addition to the 85-GHz applications revealed in this paper.

In addition to the SSM/IS, the Advanced Microwave Scanning Radiometer (AMSR) will be on board the *AQUA* platform in mid-2001 (Spencer 2000). AMSR will have channels similar to both the SSM/I and SSM/IS, but with superior spatial resolution near 5–7 km at nadir for 89 GHz due to its 2-m diameter antenna. AMSR thus represents another sensor with resolution similar to that of the TMI currently helping TC analysts worldwide. AMSR will be followed by a navy polarimetric radiometer known as the WindSat sensor (late 2002 or early 2003 launch), which will carry a 37-GHz frequency potentially useful for TC monitoring.

Multisensor data fusion opportunities will blossom when the current suite of five primary geostationary satellites used for monitoring TCs (*GOES-8*,

75°W; GOES-10, 135°W; GMS-5, 140°E; Meteosat-5, 63°E; and Meteosat-7, 0°) will be augmented with future multispectral upgrades. The GMS series will upgrade via the Meteorological Transportation Satellite (MTSAT) launch and Meteosat via the Meteosat Second Generation (MSG) satellite. The tropical cyclone community will be provided with four excellent geostationary satellites for 24 hour a day TC reconnaissance. The increased number of channels on MTSAT and MSG facilitate multichannel applications such as tracking low-level clouds at night that has shown direct applications to sheared systems with exposed low-level circulations. Enhanced scanning technology will provide more frequent TC views on these two new platforms versus the current operational sensors.

Tropical cyclone analysts desire to overlay multiple datasets in order to extract the full information content of each dataset. This is especially true for surface wind vectors from spaceborne scatterometers such as QuikSCAT. QuikSCAT was launched in June 1999 and has greatly expanded coverage with its 1800-km contiguous swath (Liu et al. 2000). Results indicate good winds and enhanced capability to detect beginning weak circulations (genesis) and delineating the radius of gale force winds, with some rain limitations. NRL-MRY will shortly add scatterometer wind overlays on top of vis/IR imagery. Successful operations of SeaWinds on QuikSCAT and the Advanced Earth Observing Satellite-II that follows will greatly improve the production of accurate surface winds around TCs globally.

The NRL-MRY demonstration via the Web has provided the operational user with a new tool to monitor TCs via passive microwave imagery. The learning process continues as the dataset expands and new insights develop. New and improved sensors are coming online and will nicely augment the existing dataset both temporally as well as with enhanced capabilities. Future opportunities are thus opening for tropical cy-

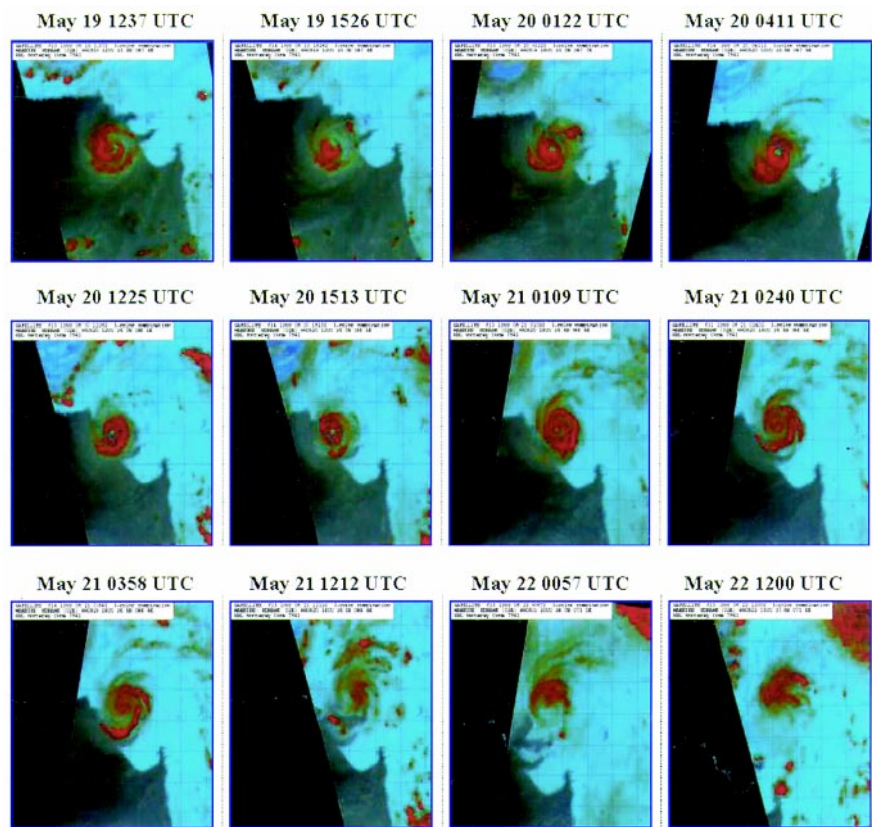


FIG. 8. SSM/I color composite sequence of images for tropical cyclone 01B in the Bay of Bengal during May 1998 (date/time label on top of each image). Image sequence starts in upper left and progresses from left to right with time and from top to bottom. Note the ability to readily follow the storm's evolution in a region that did not have ready radar access via the Internet at this time. Note that TC 01B kept its organization well inland, causing major problems.

clone applications using passive microwave data in concert with collocated data that will increase the accuracy of TC location and intensity.

Acknowledgments. Special thanks are given to the personnel of the National Hurricane Center, the Joint Typhoon Warning Center, the Naval Atlantic Meteorology and Oceanography Center in Norfolk, and the Naval Pacific Meteorology and Oceanography Center at Pearl Harbor for sending the warning and invest messages that make the Web page work in such an automated mode. We appreciate the thoughtful comments and suggestions of the reviewers and gratefully acknowledge the support of our research sponsors, the Office of Naval Research, Program Element PE-060243N, and the Space and Naval Warfare Systems Command, PMW-155 (PE-0603207N).

References

- Alishouse, J. C., S. Snyder, J. Vongsathorn, and R. Ferraro, 1990: Determination of oceanic total precipitable water from the SSM/I. *IEEE Trans. Geosci. Remote Sens.*, **28**, 811–822.

- Barrett, E. C., Ed., 1999: Tropical cyclone structure and intensity change. *Estimating the Amount of Rainfall Associated with Tropical Cyclones Using Satellite Techniques*. WMO Rep. TCP-42, 11–91.
- Connor, L. N., and P. S. Chang, 2000: Ocean surface wind retrieval using the TRMM microwave imager. *IEEE Trans. Geosci. Remote Sens.*, **38**, 2009–2016.
- Dvorak, V. F., 1984: Tropical cyclone intensity analysis using satellite data. NOAA Tech. Rep. NESDIS 11, 47 pp.
- Ferraro, R., 1997: Special Sensor Microwave Imager derived global rainfall estimates for climatological applications. *J. Geophys. Res.*, **102**, 16 715–16 735.
- Goerss, J., and R. Jeffries, 1994: Assimilation of synthetic tropical cyclone observations into the Navy Operational Global Atmospheric Prediction System. *Wea. Forecasting*, **9**, 557–576.
- Goodberlet, M. A., C. T. Swift, and J. C. Wilkerson, 1990: Ocean surface wind speed measurements of the Special Sensor Microwave/Imager (SSM/I). *IEEE Trans. Geosci. Remote Sens.*, **28**, 823–827.
- Hawkins, J., D. A. May, J. Sandidge, R. Holyer, and M. J. Helveston, 1998a: Satellite tools for monitoring tropical cyclone intensity change. Preprints, *Symp. on Tropical Cyclone Intensity Change*, Phoenix, AZ, Amer. Meteor. Soc., 51–55.
- , —, —, —, and —, 1998b: SSM/I-based tropical cyclone structural observations. Preprints, *Ninth Conf. on Satellite Meteorology and Oceanography*, Paris, France, Amer. Meteor. Soc., 230–233.
- , J. Turk and J. Haferman, 1999: Tropical cyclone structure via multiple passive microwave sensors. Preprints, *23d Conf. on Hurricanes and Tropical Cyclones*, Dallas, TX, Amer. Meteor. Soc., 178–181.
- Hollinger, J., 1989: DMSP Special Sensor Microwave/Imager calibration/validation. Final Rep. Vol. 1, Naval Research Laboratory, 153 pp. [Available from the Naval Research Laboratory, Washington, DC, 20375].
- Kummerow, C., W. Barnes, T. Kozu, J. Shiue, and J. Simpson, 1998: The Tropical Rainfall Measuring Mission (TRMM) sensor package. *J. Atmos. Oceanic Technol.*, **15**, 809–817.
- , and Coauthors, 2000: The status of the Tropical Rainfall Measuring Mission (TRMM) after two years in orbit. *J. Appl. Meteorol.*, **39**, 1965–1982.
- Lee, T. F., F. J. Turk, and K. Richardson, 1997: Stratus and fog products using GOES-8–9 3.9- μm data. *Wea. Forecasting*, **12**, 664–677.
- , J. D. Hawkins, F. J. Turk, K. Richardson, C. Sampson, and J. Kent, 1999: Tropical cyclone images now can be viewed “live” on the Web. *Eos, Trans. Amer. Geophys. Union*, **80**, 612–614.
- Liu, T. W., H. Hu, and S. Yeuh, 2000: QuikSCAT and TRMM reveal the interplay between dynamic and hydrologic parameters in Hurricane Floyd. *Eos, Trans. of Amer. Geophys. Union*, **81**, 253–257.
- Mohr, K. I., E. R. Toracinta, E. J. Zipser, and R. E. Orville, 1996: A comparison of WSR-88R reflectivities, SSM/I brightness temperatures, and lightning for mesoscale convective systems in Texas. Part II: SSM/I brightness temperatures and lightning. *J. Appl. Meteor.*, **35**, 919–931.
- Negri, A. I., R. F. Adler, and C. D. Kummerow, 1989: False-color display of Special Sensor Microwave/Imager (SSM/I) data. *Bull. Amer. Meteor. Soc.*, **70**, 146–151.
- Poe, G., 1990: Optimum interpolation of imaging microwave radiometer data. *IEEE Trans. Geosci. Remote Sens.*, **28**, 800–810.
- Sampson, R. C., and A. J. Schrader, 2000: The Automated Tropical Cyclone Forecasting System, version 3.2. *Bull. Amer. Meteor. Soc.*, **81**, 1231–1240.
- Simpson, J., C. Kummerow, W. K. Tao, and R. F. Adler, 1996: On the Tropical Rainfall Measuring Mission (TRMM). *Meteor. Atmos. Phys.*, **60**, 19–36.
- , J. Halverston, H. Pierce, C. Morales, and T. Iguchi, 1998: Eyeing the eye: Exciting early stage science results from TRMM. *Bull. Amer. Meteor. Soc.*, **79**, 1711.
- Spencer, R. W., 2000: Global climate monitoring with the EOS PM-Platform’s Advanced Microwave Scanning Radiometer (AMS-R). Preprints, *10th Conf. on Satellite Meteorology and Oceanography*, Long Beach, CA, Amer. Meteor. Soc., 479–481.
- , H. M. Goodman, and R. E. Hood, 1989: Precipitation retrieval over land and ocean with SSM/I: Identification and characteristics of the scattering signal. *J. Atmos. Oceanic Technol.*, **6**, 254–273.
- Swadley, S. D., and J. Chandler, 1991: The Defense Meteorological Satellite Program’s Special Sensor Microwave Imager/Sounder (SSM/IS). Preprints, *Seventh Symp. on Meteorological Observations and Special Session on Lower Atmospheric Studies*, New Orleans, LA, Amer. Meteor. Soc., 175–178.
- Vangasse, P., J. Charlton, and M. Jarrett, 1995: Characterization of the Advanced Microwave Sounding Unit, AMSU-B. *Adv. Space Res.*, **17**, 75–78.
- Velden, C., and K. F. Brueske, 1999: Tropical cyclone warm cores as observed from the NOAA polar orbiter satellite’s new Advanced Microwave Sounding Unit. Preprints, *23d Conf. on Hurricanes and Tropical Meteorology*, Dallas, TX, Amer. Meteor. Soc., 182–185.
- , W. S. Olsen, and B. A. Roth, 1989: Tropical cyclone center-fixing using DMSP SSM/I data. Preprints, *Fourth Conf. on Satellite Meteorology and Oceanography*, San Diego, CA, Amer. Meteor. Soc., J36–J39.

